

## HYSTERETIC BEHAVIOUR OF ELASTIC-PLASTIC BEAMS SUBJECTED TO CYCLIC BENDING

*D. Šumarac, S. Stošić*

(Received 17.01.1994)

### 1. Introduction

Problem of hysteresis is known in many areas of engineering and more generally in physics. Magnetism, adsorption, cyclic plasticity, etc., are some of them. Von Preisach (1935) [5], introduced his function in the problem of magnetism while Everett and Whitton (1952) [1], considered the problem of adsorption hysteresis. Mayergoyz (1991) [4], published monograph dealing with all aspects of Preisach model and its application in the area of magnetism. Besides its simplicity and mathematical rigour, this method has as yet to be applied in the problem of cyclic plasticity. First effort in this area is very recent. Lubarda, Šumarac and Krajčinović (1992) [2], (1993) [3], outlined basic of method applied for the axially loaded members. After that Šumarac (1993) [6] extended the model including the damage of also uniaxially loaded members. This paper is extension of the article by Šumarac and Stošić (1993) [7] dealing mostly with the cyclic plasticity of bending.

### 2. Preisach model of hysteresis

In this paragraph Preisach model for cyclic plasticity would be outlined. More detailed analysis can be found in the Mayergoyz monograph (1991) [4]. Preisach model implies the mapping of an input of strain  $\varepsilon(t)$  on the output of stress  $\sigma(t)$  in the integral form:

$$\sigma(t) = \iint_{\alpha \geq \beta} P(\alpha, \beta) G_{\alpha, \beta} \varepsilon(t) d\alpha d\beta \quad (2.1)$$

In the above formula  $G_{\alpha, \beta}$  is an elementary hysteresis operator given in Fig.1. Parameters  $\alpha$  and  $\beta$  are up and down switching values of the input.  $P(\alpha, \beta)$  is the Preisach function, i.e., a weight function of the hysteresis nonlinearity to be represented by the Preisach model.

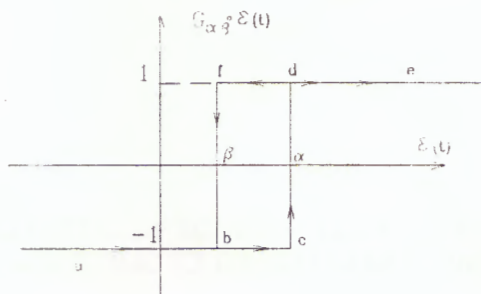


Fig.1. Elementary hysteresis operator

Integration in (2.1) is performed over the right triangle in  $(\alpha, \beta)$  plane, with line  $\alpha = \beta$  being the hypotenuse and point  $(\alpha_0; \beta = -\alpha_0)$  being the triangular vertex (Fig.2.)

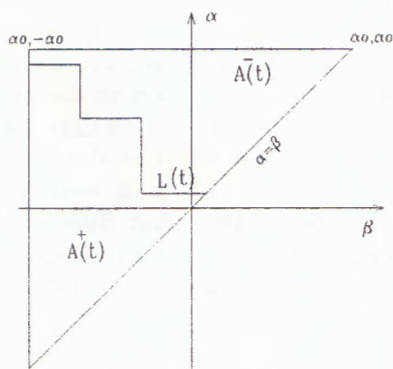


Fig.2. The limiting triangle

For a given hysteresis nonlinearity, the Preisach weight function  $P(\alpha, \beta)$  can be obtained by subsequent loading and unloading. If the input is increased to some value  $\alpha$ , the output follows the ascending branch of the major loop, and for input  $\varepsilon = \alpha$ , has the value  $f_\alpha$ . If the input is subsequently decreased to some value  $\beta$ , the output follows the corresponding (transition) curve. Denoting the output value at  $\varepsilon = \beta$  by  $f_{\alpha, \beta}$ , from the limiting triangle, it follows that:

$$f_{\alpha, \beta} - f_\alpha = -2 \int_{\beta}^{\alpha} \left( \int_{\beta'}^{\alpha} P(\alpha', \beta') d\alpha' \right) d\beta' \quad (2.2)$$

Differentiating the expression (2.2) twice, with respect to  $\alpha$  and  $\beta$ , the Preisach

weight function is derived as:

$$P(\alpha, \beta) = \frac{1}{2} \frac{\partial^2 f_{\alpha, \beta}}{\partial \alpha \partial \beta} \tag{2.3}$$

Above explained Preisach model possesses two properties. They are wiping out and congruency property. Both of them, and much more, about the model is given in the papers by Lubarda, Šumarac and Krajčinović (1992) [2], (1993) [3]. Also, in the mentioned papers, several combinations of elastic and slip element are considered. In this paper only elastic-ideally plastic material will be considered.

Elastic-ideally plastic material can be modeled by a series of a slip element (with yield strength  $Y$ ) and an elastic element (with modulus  $E$ ), (Fig.3).

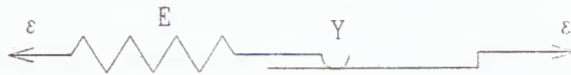


Fig.3. Single elastic-ideally plastic element

To formulate the Preisach representation for the hysteretic behavior of this material, consider the strain input  $\varepsilon(t)$  ranging quasistatically between extreme values  $\varepsilon_0$  and  $-\varepsilon_0$ . From the major hysteresis loop and transition curves (lines), shown in (Fig.4.), it then follows that  $f_\alpha = Y$  and,

$$f_{\alpha, \beta} = \begin{cases} Y - E(\alpha - \beta) & \text{for } \alpha - 2Y/E \leq \beta \leq \alpha \\ -Y & \text{for } \beta < \alpha - 2Y/E \\ Y & \text{for } \beta > \alpha \end{cases} \tag{2.4}$$

Differentiating (2.4) with respect to  $\beta$  leads to:

$$\frac{\partial f_{\alpha, \beta}}{\partial \beta} = E \left[ H(\alpha - \beta) - H\left(\alpha - \beta - 2\frac{Y}{E}\right) \right] \tag{2.5}$$

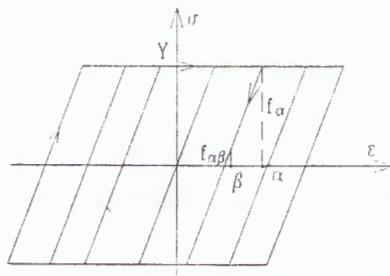


Fig.4. A major hysteresis loop and several transition lines

Substituting (2.5) into (2.3) yields to the Preisach function:

$$P(\alpha, \beta) = \frac{E}{2} \left[ \delta(\alpha - \beta) - \delta\left(\alpha - \beta - 2\frac{Y}{E}\right) \right] \quad (2.6)$$

The Preisach function has support only along the two parallel lines:  $\alpha - \beta = 0$  and  $\alpha - \beta = 2Y/E$ , vanishing in the rest of the limiting triangle. Once the expression (2.6) is known, the expression (2.1) is sufficient to obtain the stress as a function of time for a prescribed history of strain in a single element.

For a system consisting of infinitely many of these elements (with randomly distributed yield strength) connected in a parallel (Fig.5), the overall stress is:

$$\sigma(t) = \int_{Y_{\min}}^{Y_{\max}} p(Y) \sigma(Y, t) dY \quad (2.7)$$

where  $\sigma(Y, t)$  is the stress in an individual element (unit) given by (2.1) and having a yield strength within the range  $Y_{\min} < Y < Y_{\max}$ . Also in the expression (2.1), for the Preisach function, the expression (2.6) has to be substituted. Function  $p(Y)$  is the yield strength probability density function. Taking uniform distribution of yield strength it follows:

$$p(Y) = \frac{1}{Y_{\max} - Y_{\min}} \quad (2.8)$$

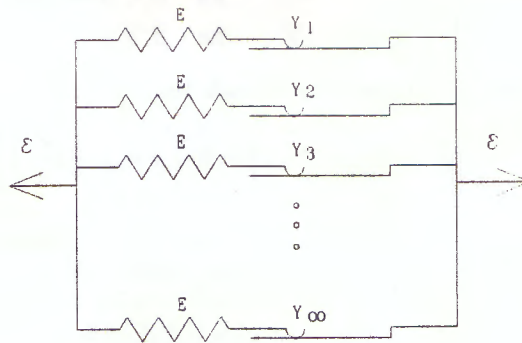


Fig.5. Parallel connection of infinitely many ideally elasto-plastic elements

Substituting (2.8) into (2.7) and taking (2.1) and (2.6) it follows:

$$\sigma(t) = \frac{E}{2} \left( \int_{-\varepsilon_0}^{\varepsilon_0} G_{\alpha, \alpha} \varepsilon(t) d\alpha - \frac{1}{Y_{\max} - Y_{\min}} \iint_A G_{\alpha, \beta} \varepsilon(t) d\alpha d\beta \right) \quad (2.9)$$

where the integration domain  $A$  is represented by the shaded band area of the limiting triangle (Fig.6).

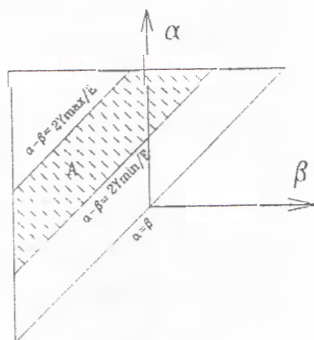


Fig.6. Limiting triangle with the band area providing support for Preisach function

The associated Preisach function for the entire system is:

$$P(\alpha, \beta) = \frac{E}{2} \left\{ \delta(\alpha - \beta) - \frac{E}{2} \frac{1}{Y_{\max} - Y_{\min}} \left[ H \left( \alpha - \beta - 2 \frac{Y_{\min}}{E} \right) - H \left( \alpha - \beta - 2 \frac{Y_{\max}}{E} \right) \right] \right\} \quad (2.10)$$

### 3. Cyclic bending

Cyclic bending is in a nature one dimensional state of stress also. In that sense already explained procedure would not be difficult to be extended. Assuming wide spread Bernoulli's hypothesis about plane cross section, the strain at any distance from the neutral fiber is:

$$\varepsilon(y, t) = \kappa(t) \cdot y \quad (3.1)$$

Substituting (3.1) into (2.1) it follows:

$$\sigma(y, t) = \iint_{\alpha \geq \beta} P(\alpha, \beta) G_{\alpha, \beta}(\kappa(t) y) d\alpha d\beta \quad (3.2)$$

In the above formula, integration is performed on every triangle that is dependent of the distance from the neutral fiber. Instead of one triangle that represents the whole cross section, now every level  $y$  is represented by one limiting triangle. In the other words, in this way the prism with triangular base, and hereafter will be referred to as "Preisach prism", is obtained, Fig.7.

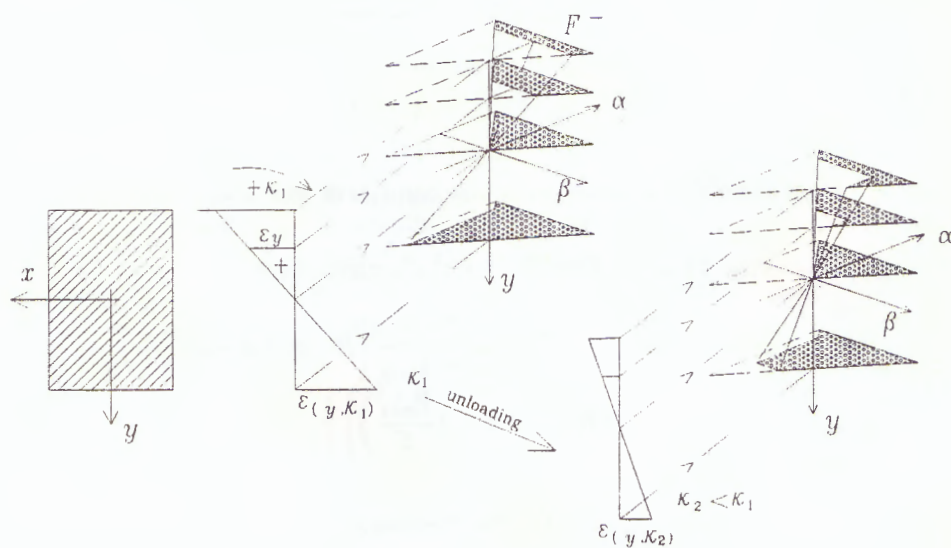


Fig.7. "Preisach prism" for cyclic bending

The moment curvature relation for a rectangular cross section is obtained by integration in the form:

$$M(t) = \int_{-\frac{h}{2}}^{\frac{h}{2}} y \sigma(y, t) b(y) dy \quad (3.3)$$

From (3.3), using (2.9) it further follows:

$$M(t) = \int_{-\frac{h}{2}}^{\frac{h}{2}} yb(y) \frac{E}{2} \left( \int_{-\epsilon_0}^{\epsilon_0} G_{\alpha,\alpha}(y\kappa(t)) d\alpha - \frac{E}{2(Y_{\max} - Y_{\min})} \iint_A G_{\alpha,\beta}(y\kappa(t)) d\alpha d\beta \right) dy \quad (3.4)$$

If the cross section is unsymmetric, than the axial force is:

$$N(t) = \int_a^b \sigma(y,t)b(y) dy \quad (3.5)$$

or, substituting (2.9) into (3.5) it is obtained:

$$N(t) = \int_a^b b(y) \frac{E}{2} \left( \int_{-\epsilon_0}^{\epsilon_0} G_{\alpha,\alpha}(y\kappa(t)) d\alpha - \frac{E}{2(Y_{\max} - Y_{\min})} \iint_A G_{\alpha,\beta}(y\kappa(t)) d\alpha d\beta \right) dy \quad (3.6)$$

where  $a$  and  $b$  are the distances from the center of the gravity to the lower and upper fiber of the cross section. Once the expression (3.4) and (3.6) are known, the moment curvature relation, and axial force axial deformation is straightforward.

If the axial strain  $\epsilon(t)$  at the center of gravity of the cross section is prescribed, besides the curvature change  $\kappa(t)$ , then the strain at any distance from the line of the center of gravity is given by:

$$\epsilon(y,t) = \epsilon(t) + \kappa(t)y \quad (3.7)$$

The expression (3.7) should be then replaced in the expression (2.1), and all subsequent expressions could be easily rederived.

#### 4. Numerical examples

To show the application of the above explained procedure, several numerical examples would be presented. First a rectangular cross section under pure bending will be outlined. Then a triangular cross section, as the example of the unsymmetrical shape, under pure bending will be considered. Finally the rectangular cross section, under cyclic axial strain of the line of the center of gravity and cyclic curvature change will be outlined.

#### 4.1. Rectangular Cross Section under Pure Bending

Consider a rectangular cross section given in Fig.8 a).

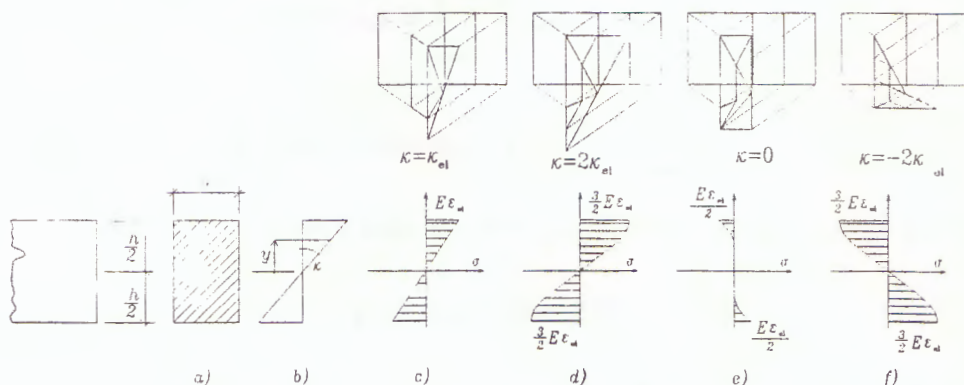


Fig.8. Rectangular cross section under pure bending

Let the cross section be loaded with the curvature change that is prescribed as in Fig.9.

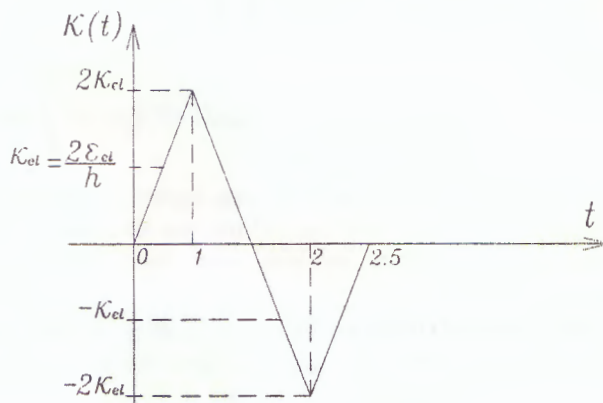


Fig.9. Cyclic curvature change

In the region  $0 < t < 0.5$ , or,  $0 < \kappa < \kappa_{el}$  where  $\kappa_{el} = 2\varepsilon_{el}/h$ , all fibers of the cross section are in the elastic region, and the stress is:

$$\sigma(y, t) = E \kappa(t) y \quad (4.1)$$

The diagram of stress, given by (4.1), and governing "Preisach prism" is plotted in Fig.8 c). Substituting (4.1) into (3.3) the moment curvature relation is obtained as:

$$M(t) = E I \kappa(t) \quad (4.2)$$

where  $I = bh^3/12$  is moment of inertia of the rectangular cross section. If the curvature is further increased (region  $0.5 < t < 1$ ), then the nonlinear behavior



will appear, and the stress in the fiber at the distance  $y$  is:

$$\sigma(y, t) = E \varepsilon_{el} \left[ \frac{2\kappa(t) y}{\kappa_{el} h} - H \left( y - \frac{\varepsilon_{el}}{\kappa} \right) 2 \left( \frac{\kappa(t) y}{\kappa_{el} h} - \frac{1}{2} \right)^2 \right] \quad (4.3)$$

where  $H$  stands for Heaviside function. The stress (4.3) is given in Fig.8 d) for  $\kappa(t = 1.0) = 2\kappa_{el}$ . Substituting (4.3) into (3.3) it is obtained:

$$M(t) = EI \kappa(t) - 3EI \kappa_{el} \left[ \frac{1}{8} \frac{\kappa(t)^2}{\kappa_{el}^2} \left( 1 - \frac{\kappa_{el}^4}{\kappa(t)^4} \right) - \frac{1}{3} \frac{\kappa(t)}{\kappa_{el}} \left( 1 - \frac{\kappa_{el}^3}{\kappa(t)^3} \right) + \frac{1}{4} \left( 1 - \frac{\kappa_{el}^2}{\kappa(t)^2} \right) \right] \quad (4.4)$$

From (4.4) for  $\kappa = \kappa_{el}$ ,  $M = EI \kappa_{el}$  and for  $\kappa = 2\kappa_{el}$ ,  $M = 1.78125 EI \kappa_{el}$ . The shape of the "Preisach prism" for  $\kappa = 2\kappa_{el}$  is presented in Fig.8 d). For  $1 < t < 1.5$ , or  $0 < \kappa < 2\kappa_{el}$ , the unloading starts. The "Preisach prism" doesn't change at all. Change takes place only along the hypotenuse and so the response is elastic. The stress is given by:

$$\sigma(y, t) = E \varepsilon_{el} \left[ 2 \frac{\kappa(t) y}{\kappa_{el} h} - H \left( y - \frac{h}{4} \right) 2 \left( 2 \frac{y}{h} - \frac{1}{2} \right)^2 \right] \quad (4.5)$$

From (4.5) for  $\kappa = 0$  the "residual stress" is:

$$\sigma(y, t = 1.5) = -E \varepsilon_{el} H \left( y - \frac{h}{4} \right) 2 \left( 2 \frac{y}{h} - \frac{1}{2} \right)^2 \quad (4.6)$$

and it is plotted in Fig.8 e). The moment-curvature relation in this region is from (4.5) and (3.3) given by:

$$M(t) = EI \kappa_{el} \left[ \frac{\kappa(t)}{\kappa_{el}} - \frac{7}{32} \right] \quad (4.7)$$

It is easy to see that the response is elastic. The residual stresses are very important issue in all area of engineering, specially in civil and mechanical engineering. If the curvature changes the sign, for  $1.5 < t < 2$ , or  $-2\kappa_{el} < \kappa < 0$ , the Preisach prism is shown in Fig.8 f), and the stress function is:

$$\sigma(y, t) = E \varepsilon_{el} \left\{ 2 \frac{\kappa(t) y}{\kappa_{el} h} - H \left( y - \frac{h}{4} \right) 2 \left( 2 \frac{y}{h} - \frac{1}{2} \right)^2 + H(y - y_*) \left[ \frac{\kappa(t) y}{\kappa_{el} h} - 2 \left( \frac{y}{h} - 1 \right) \right]^2 \right\} \quad (4.8)$$

In the above formula  $y_*$ , is given by:

$$y_* = \frac{h}{2} \frac{2\kappa_{el}}{2\kappa_{el} - \kappa(t)} \quad (4.9)$$

In Fig.8 f) the diagram of the stress given by (4.8), for  $\kappa = -2\kappa_{el}$  is plotted to. The moment curvature relation, from (4.8) and (3.3) is:

$$M(t) = EI \kappa_{el} \left[ \frac{\kappa(t)}{\kappa_{el}} - \frac{7}{32} + 3 \left( \frac{\kappa(t)}{\kappa_{el}} - 2 \right)^2 \left( \frac{1}{16} - \frac{\kappa_{el}^4}{(2\kappa_{el} - \kappa(t))^4} \right) + 8 \left( \frac{\kappa(t)}{\kappa_{el}} - 2 \right) \left( \frac{1}{8} - \frac{\kappa_{el}^3}{(2\kappa_{el} - \kappa(t))^3} \right) + 6 \left( \frac{1}{4} - \frac{\kappa_{el}^2}{(2\kappa_{el} - \kappa(t))^2} \right) \right] \quad (4.10)$$

In the same manner for the future steps the procedure is obvious. The hysteresis loop  $M - \kappa$ , for prescribed history of  $\kappa(t)$  given in Fig.9, is plotted in Fig.10.

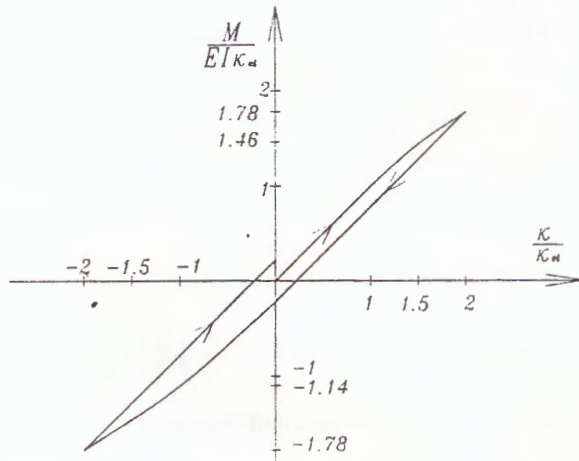


Fig.10. Hysteresis loop  $M - \kappa$  for rectangular cross section due to curvature change shown in Fig.9.

From Fig.10. it could be easily seen that the Preisach model satisfies Bauschinger's effect.

#### 4.2. Triangular Cross Section under Pure Bending

In this subsection a triangular cross section given in Fig.11. under pure bending would be presented.

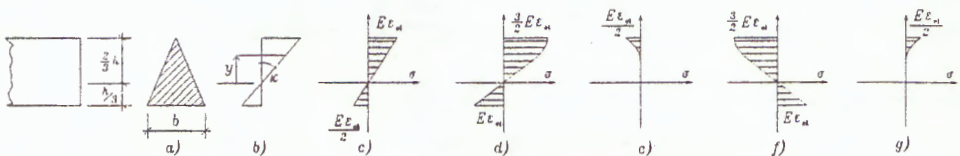


Fig.11. Triangular cross section under pure bending

For the history of curvature change already shown in the preceding example the diagram of the stress in the cross section at any time instant and the moment-curvature relation would be given. In the region  $0 < t < 0.5$ , or  $0 < \kappa < \kappa_{el}$ , where  $\kappa_{el} = 3\varepsilon_{el}/2h$  whole cross section is in elastic region, and the stress is given by:

$$\sigma(y, t) = E \kappa(t)y \quad (4.11)$$

while from (4.11), (3.3) and (3.6) moment and normal force are:

$$M(t) = E I \kappa(t) \quad (4.12)$$

$$N(t) = 0. \quad (4.13)$$

Expression (4.13) shows that in the elastic region for pure bending of unsymmetrical cross section there is no axial force. The expression (4.11) is plotted in Fig.11 c). In the region  $0.5 < t < 1$ , or  $\kappa_{el} < \kappa < 2\kappa_{el}$ , upper fiber is in the plastic region, and the stress in any fiber is given by:

$$\sigma(y, t) = E \varepsilon_{el} \left[ \frac{3 \kappa(t) y}{2 \kappa_{el} h} - H \left( y - \frac{\varepsilon_{el}}{\kappa(t)} \right) \frac{1}{2} \left( \frac{3 \kappa(t) y}{2 \kappa_{el} h} - 1 \right)^2 \right] \quad (4.14)$$

The expression (4.14) is plotted in Fig.11 d) for  $\kappa = 2\kappa_{el}$ . Substituting (4.14) into (3.3) and (3.5), with the proper limits of integration, it is obtained:

$$M(t) = E I \kappa(t) \left[ 1 - \frac{16}{27} \left( -1 + \frac{\kappa_{el}}{\kappa(t)} + \frac{3 \kappa(t)}{10 \kappa_{el}} - \frac{1}{2} \frac{\kappa_{el}^3}{\kappa(t)^3} + \frac{1}{5} \frac{\kappa_{el}^4}{\kappa(t)^4} \right) \right] \quad (4.15)$$

$$N(t) = E \varepsilon_{el} b \frac{h}{2} \left[ -\frac{2}{9} + \frac{4}{27} \left( \frac{\kappa_{el}}{\kappa(t)} + \frac{\kappa(t)}{\kappa_{el}} \right) - \frac{1}{27} \left( \frac{\kappa_{el}^2}{\kappa(t)^2} + \frac{\kappa(t)^2}{\kappa_{el}^2} \right) \right] \quad (4.16)$$

For  $\kappa = \kappa_{el}$  from (4.15) and (4.16) it is obtained:  $M = E I \kappa_{el}$ ,  $N = 0$ , while for  $\kappa = 2\kappa_{el}$ ,  $M = 1.9407 E I \kappa_{el}$ , and  $N = -E b h \varepsilon_{el}/216$ . Above consideration shows that in the case of unsymmetrical cross section, even for pure bending, in plastic range there is axial force. In the other words, if the neutral axis is fixed at the center of gravity of the cross section, then the stresses due to pure bending are unbalanced.

For the sake of completeness, we will derive the stresses for whole cycle. For unloading  $1 < t < 1.5$  or  $0 < \kappa < 2\kappa_{el}$ , unloading takes place. The stress is then given by:

$$\sigma(y, t) = E \varepsilon_{el} \left[ \frac{3 \kappa(t)}{2 \kappa_{el}} - H \left( y - \frac{h}{3} \right) \frac{1}{2} \left( 3 \frac{y}{h} - 1 \right)^2 \right] \quad (4.17)$$

For  $\kappa = 0$  the stress reads:

$$\sigma(y, t) = -E \varepsilon_{el} H \left( y - \frac{h}{3} \right) \frac{1}{2} \left( 3 \frac{y}{h} - 1 \right)^2 \quad (4.18)$$

The expression (4.18) is plotted in Fig.11 e) and it represents again the residual stress. From diagram of stress it could be easily seen that the axial force is

different from zero. For the further decrease of the curvature, upper fiber will be in compression, i.e., for  $1.5 < t < 2$ , or  $-2\kappa_{el} < \kappa < 0$ , the stress is given by:

$$\sigma(y, t) = E \varepsilon_{el} \left\{ \frac{3 \kappa(t) y}{2 \kappa_{el} h} - H \left( y - \frac{h}{3} \right) \frac{1}{2} \left( 3 \frac{y}{h} - 1 \right)^2 + H(y - y_{*1}) \left[ \frac{3 \kappa(t) y}{4 \kappa_{el} h} + \frac{3}{2} \left( \frac{y}{h} - \frac{2}{3} \right) \right]^2 \right\} \quad (4.19)$$

where

$$y_{*1} = \frac{2}{3} h \frac{2\kappa_{el}}{2\kappa_{el} - \kappa(t)} \quad (4.20)$$

For  $\kappa = -2\kappa_{el}$ ,  $y_{*1} = \frac{2}{3}h$ , the stress is given by:

$$\sigma(y, t) = E \varepsilon_{el} \left\{ -3 \frac{y}{h} - H \left( y - \frac{h}{3} \right) \left\{ \frac{1}{2} \left( 3 \frac{y}{h} - 1 \right)^2 - \left[ -\frac{3y}{2h} + \frac{3}{2} \left( \frac{y}{h} - \frac{2}{3} \right) \right]^2 \right\} \right\} \quad (4.21)$$

The expression (4.21) is plotted in Fig.11 f). Finally for  $-2\kappa_{el} < \kappa < 0$  or  $2 < t < 2.5$ , the stress is given by:

$$\sigma(y, t) = E \varepsilon_{el} \left\{ \frac{3 \kappa(t) y}{2 \kappa_{el} h} - H \left( y - \frac{h}{3} \right) \left\{ \frac{1}{2} \left( 3 \frac{y}{h} - 1 \right)^2 - \left[ -\frac{3y}{2h} + \frac{3}{2} \left( \frac{y}{h} - \frac{2}{3} \right) \right]^2 \right\} \right\} \quad (4.22)$$

From (4.22) for  $\kappa = 0$  the "residual stress" is:

$$\sigma(y, t) = -E \varepsilon_{el} H \left( y - \frac{h}{3} \right) \left\{ \frac{1}{2} \left( 3 \frac{y}{h} - 1 \right)^2 - \left[ -\frac{3y}{2h} + \frac{3}{2} \left( \frac{y}{h} - \frac{2}{3} \right) \right]^2 \right\} \quad (4.23)$$

The expression (4.23) is plotted in Fig.11 g).

### 4.3. Rectangular cross section under axial stretching and bending

In the preceding subsection we had the case where the axial force and bending moment appear due to unsymmetrical cross section even for the pure bending. The same problem is for symmetrical cross section under axial stretching and pure bending. Consider a rectangular cross section, as shown in Fig.8, under the curvature and axial stretching change as shown in Fig.12.

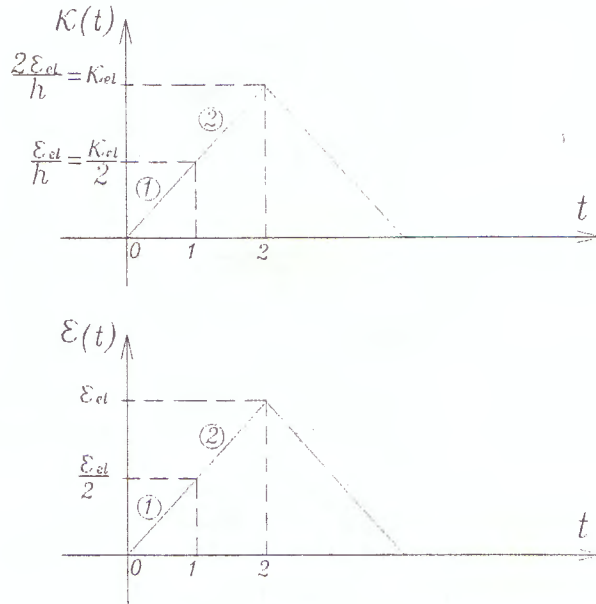


Fig. 12. History of curvature and axial stretching change

In the region  $0 < t < 1$  from the expression (3.6) and (3.1) it is obtained:

$$\sigma(y, t) = E \epsilon_{el} \left( \frac{\epsilon(t)}{\epsilon_{el}} + 2 \frac{\kappa(t) y}{\kappa_{el} h} \right) \quad (4.24)$$

The linear distribution of stress given by (4.24) is shown in Fig. 13 b). The moment and axial force are easily obtained by integration:

$$N(t) = E b h \epsilon(t) \quad (4.25)$$

$$M(t) = E I \kappa(t) \quad (4.26)$$

If the axial stretching and pure bending is further increased (region  $1 < t < 2$ ), the stress is:

$$\sigma(y, t) = E \epsilon_{el} \left[ \frac{2\kappa(t) y}{\kappa_{el} h} + \frac{\epsilon(t)}{\epsilon_{el}} - H \left( y - \frac{\epsilon_{el} - \epsilon(t)}{\kappa(t)} \right) 2 \left( \frac{\kappa(t) y}{\kappa_{el} h} + \frac{1}{2} \frac{\epsilon(t)}{\epsilon_{el}} - \frac{1}{2} \right)^2 \right] \quad (4.27)$$

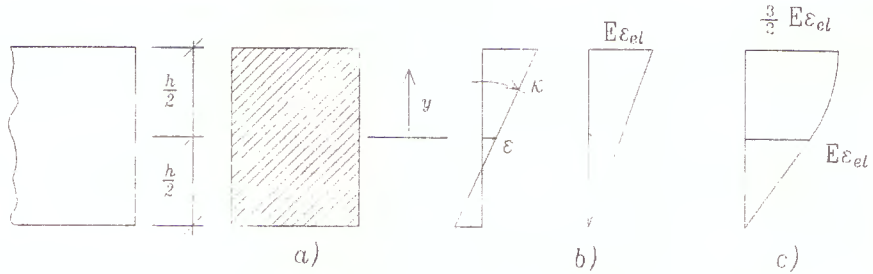


Fig. 13 Rectangular cross section under axial stretching and bending

The diagram of stress given by (4.27) is plotted in Fig.13 c). Substituting (4.27) into (3.3) and (3.6) it follows:

$$N(t) = E b h \left[ \varepsilon(t) - 2\varepsilon_{el} \left( \frac{1}{12} \frac{\kappa(t)^2}{\kappa_{el}^2} + \frac{1}{4} \frac{\varepsilon(t)^2}{\varepsilon_{el}^2} + \frac{1}{4} - \frac{1}{2} \frac{\varepsilon(t)}{\varepsilon_{el}} \right) \right] \quad (4.28)$$

$$M(t) = E \varepsilon_{el} b \left\{ \frac{2\kappa(t) h^3}{\kappa_{el} 12} - 2 \left\{ \left[ \frac{h^3}{8} - \left( \frac{\varepsilon_{el} - \varepsilon(t)}{\kappa(t)} \right)^3 \right] \frac{\kappa(t)}{3h\kappa_{el}} \left( \frac{\varepsilon(t)}{\varepsilon_{el}} - 1 \right) + \left[ \frac{h^4}{32} - \left( \frac{\varepsilon_{el} - \varepsilon(t)}{\kappa(t)} \right)^4 \right] \frac{\kappa(t)^2}{4h^2\kappa_{el}^2} + \left[ \frac{h^2}{4} - \left( \frac{\varepsilon_{el} - \varepsilon(t)}{\kappa(t)} \right)^2 \right] \frac{1}{8} \left( \frac{\varepsilon(t)}{\varepsilon_{el}} - 1 \right)^2 \right\} \right\} \quad (4.29)$$

The further consideration is straightforward.

## 5. Conclusion

In the present study application of Preisach model, already successfully implemented for axially loaded members, is extended to the cyclic bending of elasto-plastic beams. Due to arbitrary axial stretching and curvature change during the time, the stress, axial forces and moments are calculated for symmetrical (rectangular) and unsymmetrical (triangular) cross sections. The model starts from well known elements of the classical theory of plasticity, Hooke's (spring) and St. Venant (slider) elements, and using Preisach approach gives the closed form analytical solution for arbitrary history of loading. The hysteresis loop  $M - \kappa$  and residual stresses, very important in engineering design, are calculated. The model satisfies Bauschinger's effect, already very well known in cyclic plasticity.

**Acknowledgement.** The authors gratefully acknowledge the financial support provided by the Scientific Fund of Serbia, to the University of Belgrade, Department of Civil Engineering, through the grant number 1704, which made this work possible.

## REFERENCES

- [1] Everett, D.H., and Whitton, W.I., *A General Approach to Hysteresis*, *Trans. Faraday Soc.*, Vol.48 (1952), 749-757.
- [2] Lubarda, A. V., Šumarac, D., Krajčinović, D., *Hysteretic response of ductile materials subjected to cycling loads*, Recent Advances in Damage Mechanics and Plasticity, JU,J.W. Ed.,145-157, ASME Publication, AMD-Vol.123, New York, (1992).
- [3] Lubarda, A. V., Šumarac, D., Krajčinović, D., *Preisach Model and Hysteretic Behavior of Ductile Materials*, *Eur. J. Mech. A / Solids*, 12, No. 4 (1993), 445-470.
- [4] Mayergoyz, I.D., *Mathematical Models of Hysteresis*, Springer-Verlag, New York, (1991).
- [5] Preisach, F., *Über die magnetische Nachwirkung*, *Z. Phys.* 94 (1935), 277-302.
- [6] Šumarac D., *Hysteretic behavior of elasto-plastic materjals* (in Serbian), Structural analysis - Recent topics of nonlinear analysis, Ed. M.Sekulović, Građevinska knjiga, Beograd (1992), 139-163.
- [7] Šumarac, D., Stošić, S., *Cyclic bending of elasto-plastic beams* (in Serbian), Proc. of XX YU Congress of Appl. and Theor. Mechanics, Kragujevac, (1993).

## ГИСТЕРЕЗИСОВОЕ ПОВЕДЕНИЕ УПРУГОПЛАСТИЧЕСКИХ БАЛОК ПОДВЕРЖЕННЫХ ЦИКЛИЧЕСКОМ ИЗГИБЕ

В настоящей работе изучается циклический изгиб упругопластических балок. Работа представляет расширение использования модели Прайзака, уже успешно использованного для осевой нагрузки стержня, на изгиб балок. Пользуясь этой моделью показано что получается точное аналитическое решение для напряжения, осевой силы и изгибающего момента в поперечном сечении для любой, заданной, истории деформаций и изменения кривизны. При этом мы пошли от основных тел (Гука и Сен Венаня) хорошо знакомых в теории пластичности. В работе показано как можно конструировать петли гистерезиса  $M - \kappa$ , для заданного циклического изменения кривизны, и получить остаточные напряжения, очень важные в инженерных применениях.

## HISTEREZISNO PONAŠANJE ELASTO-PLASTIČNIH GREDA IZLOŽENIH CIKLIČNOM SAVIJANJU

U posmatranom radu proučava se ciklično savijanje grednih nosača u elasto-plastičnoj oblasti. Rad predstavlja proširenje primene Prajakovog modela na savijanje grednih nosača u odnosu na aksijalno naprezanje, već opisano u literaturi. Primenom ovog modela prikazano je da se dobijaju tačna analitička rešenja za napon, normalnu silu i momenat savijanja u poprečnom preseku grede za zadatu istoriju promene krivine i dilatacije u osi nosača. Pri tome se polazi od osnovnih tela (Hukovog i Sen-Venanovog) dobro poznatih u teoriji plastičnosti. U radu je pokazano kako se može konstruisati histerezisna petlja  $M-k$  za zadatu cikličnu promenu, i izračunati zaostali naponi u bilo kom trenutku vremena, vrlo važni u inženjerskim primenama.

Dragoslav Šumarac, Saša Stošić  
Civil Engineering, University of Belgrade,  
Bul. Revolucije 73  
11000 Belgrade, Yugoslavia